Chinese Journal of Physiology 51(6): 376-386, 2008

Synergic Co-Activation of Muscles in Elbow Flexion *via* Fractional Brownian Motion

Shyang Chang[1], Ming-Chun Hsyu[1], Hsiu-Yao Cheng[2], and Sheng-Hwu Hsieh[3]

[1]*Department of Electrical Engineering, National Tsing Hua University, Hsinchu 300*
[2]*Department of Chemistry, Tunghai University, Taichung 407*
and
[3]*Department of Endocrinology and Metabolism, Chang Gung Memorial Hospital, Chang Gung University College of Medicine, Taoyuan 333, Taiwan, ROC*

Abstract

In reflex and volitional actions, co-activations of agonist and antagonist muscles are believed to be present. Recent studies indicate that such co-activations can be either *synergic* or *dyssynergic*. The aim of this paper is to investigate if the co-activations of biceps brachii, brachialis, and triceps brachii during volitional elbow flexion are in the synergic or dyssynergic state. In this study, two groups with each containing six healthy male volunteers participated. Each person of the first group performed 30 trials of volitional elbow flexion while each of the second group performed 30 trials of passive elbow flexion as control experiments. Based on the model of fractional Brownian motion, the *intensity* and *frequency* information of the surface electromyograms (EMGs) could be extracted simultaneously. No statistically significant changes were found in the control group. As to the other group, results indicated that the surface EMGs of all five muscle groups were temporally synchronized in *frequencies* with persistent *intensities* during each elbow flexion. In addition, the mean values of fractal dimensions for rest and volitional flexion states revealed significant differences with $P < 0.01$. The obtained positive results suggest that these muscle groups work together synergically to facilitate elbow flexion during the co-activations.

Key Words: synergic co-activation of elbow flexion, synergy of coupled muscles, fractional Brownian motion, fractal dimension, reciprocal inhibition, synchronization of rhythms

Introduction

It was believed that the coordinated activities like volitional flexion of elbow and other reflexes displayed reciprocal innervations of antagonistic muscles (40). For instance, in the flexion of the elbow joint, the triceps was thought to relax and the biceps was in active contraction. That is, one muscle of an antagonistic couple was thrown out of action while the other was brought into action. This concept was later referred to as reciprocal inhibition (4, 6, 22, 28, 30, 36, 37, 44).

There were, on the other hand, instances of the co-activations of forearm antagonist muscles of monkeys (21) and hind limb muscles of frogs during kicking (14, 15, 43), showing that these co-activations were related to movement kinematics. Meanwhile, different methods to extract the co-activation information from electromyograms (EMGs) were also proposed (5, 19). One other interesting example in physiology was the micturition reflex. The external urethral sphincter was believed to relax while the bladder was active during voiding (1, 2, 13, 39, 42, 46). Thus, the central nervous system maintained a reciprocal inhibition between the bladder parasympathetic efferents and the motoneurons innervating the external urethral sphincter. However, recent studies indicated that the external urethral sphincter was not relaxed but co-

Corresponding author: Dr. S. Chang, Department of Electrical Engineering, National Tsing Hua University, Hsinchu 300, Taiwan, ROC. Tel: +886-35731146, Fax: +886-35715971, E-mail: shyang@ee.nthu.edu.tw
Received: March 24, 2008; Revised: July 21, 2008; Accepted: July 25, 2008.
 ISSN : 0304-4920. http://www.cps.org.tw

activated with the detrusor of bladder during micturition for both normal and spinal-cord injured female Wistar rats. The only difference between these two types of co-activation was that the external urethral sphincter was in fact *synergically* co-activated with the bladder for normal rats and *dyssynergically* co-activated for the spinal-cord injured rats (9-12). Most recently, the investigation of forearm pronation also indicated that coupled muscle groups for normal subjects were under synergic co-activation while for patients with radial palsy were under dyssynergic co-activation (8). Hence, it would be fitting for us to investigate if the dynamic interaction among human muscles during elbow volitional flexion could also be in synergic co-activation.

Notice that in order to analyze the multi-channel EMG signals, various sophisticated methods were proposed (3, 14, 15, 17, 27, 29, 31, 34). However, to extract both the spatio-temporal *frequencies* and signal *intensities* from the surface EMGs of involved muscles during volitional elbow flexion, the fractional Brownian motion (FBM) model (7-11) would be invoked. The advantages and comparisons of FBM with other methods could be accessed through the aforementioned references. In the following section, we would try to supply the rationale and the mathematical background behind this FBM approach.

Mathematical Framework of FBM

It is well-known that biological or physiological rhythms are usually buried in random noise and the muscular activities are the end results of activities of many thousands of muscle fibers. In addition, muscular signals can also exhibit the power-law correlation (8-12, 25). Hence, it is imperative to extract the intensities and frequencies of EMGs (8-12, 18, 20, 23, 26, 45). In this paper, the descriptive term of describing coupled muscle groups being "*synchronized*" is used to denote that they all have the *same frequencies* during action. The term of coupled muscle groups being "*synergic*" is used to denote that they have both the *same frequencies* and persistent signal *intensities* in their noise-like EMGs (8). The importance of having the same frequencies with persistent intensities is equivalent to being synchronized with strength in physiological locomotion or other important functions (8, 9, 11, 24).

The rationale behind our FBM approach could be dated back to the following discovery in 1828.

Brownian Motion

Robert Brown reported the observation of irregular movement of pollen grains and inorganic particles suspended in water that year. Albert Einstein, in 1905, then gave a quantitative treatment to this irregular movement. However, the rigorous mathematical construction of this movement was not proposed until 1930s by Norbert Wiener (38).

According to him, the Brownian motion $B(t)$ was defined formally as the integral of an infinite series of oscillations with random amplitudes as follows.

$$B(t) = \int_0^t \sum_{n=-\infty}^{\infty} \xi_n e^{inx} dx , \qquad [1]$$

where $\{\xi_n\}$ is a sequence of independent, identically distributed standard Gaussian random variables (38). This integral converges almost surely and in the L^2 sense. In physiological applications, the Brownian motion provides a good model for the stochastic cumulative effects of many muscle fibers under different oscillation frequencies with random amplitudes (9-11). It is worth noting that the increments of Brownian motion are stationary and independent. However, empirical studies often suggested the existence of strong dependence between samples in applications. Thus, B. Mandelbrot proposed in 1968 the FBM with correlated increments for applications in real environment (35). The following material on FBM could be found in many literatures. We included them here for the sake of completeness.

FBM (35)

The FBM $\{B_H(t), t \geq 0\}$ with the Hurst parameter H $(0 < H < 1)$ and starting value b_0 at time 0 was defined by $B_H(0) = b_0$, and

$$B_H(t) - B_H(0)$$

$$= \frac{1}{\Gamma(H + 1/2)} \left\{ \int_{-\infty}^{0} [(t-s)^{H-1/2} - (-s)^{H-1/2}] dB(s) \right.$$

$$\left. + \int_0^t (t-s)^{H-1/2} dB(s) \right\} . \qquad [2]$$

The increments of this FBM are now still stationary but dependent. The discrete-time fractional Gaussian noise (DFGN) process $\{x_H[n]\}$ is derived from the increment of such sampled FBM. That is, $x_H[n] = B_H[n] - B_H[n-1]$ where $B_H[n] = B_H[nT_s]$ and T_s is the sampling period. The autocorrelation function of a DFGN process, denoted by $r_H[k]$, can be evaluated by the following formula:

$$E(x_H[n+k]x_H[n])$$

$$\equiv r_H[k] = \frac{1}{2}(|k+1|^{2H} - 2|k|^{2H} + |k-1|^{2H}). \qquad [3]$$

The FBM is clearly reduced to Brownian motion when $H = 1/2$. Hence, the FBM can be visualized as a generalization of the Brownian motion. In our

applications, the detailed rationale behind modeling the surface EMG signals as FBM can be found in (8). Hence, the sampled version of the surface EMG signals could be modeled as discrete-time fractional Brownian motion (DFBM) (8-11, 32). It is also clear from equations [2] and [3] that the DFGN can be invoked to find the Hurst parameter H of DFBM. The FD is defined as $D = 2 - H$. Its physical meaning is explained below.

The Meaning of FDs in Physiological Signals (8)

Since the signal intensities of physiological rhythms in EMGs are usually low and are buried in random-like noise, one cannot use directly the *raw* signal amplitudes that are contaminated by noise. Instead, we have to eliminate the effects of noise and try to obtain the "signal intensity" from the covariance function. The covariance function of FBM can be computed as $\langle (B_H(t))^2 \rangle \sim t^{2H}$. Here the term $\langle (B_H(t))^2 \rangle$ is equivalent to the average "signal intensity" and it is proportional to H and inversely to the corresponding $D = 2 - H$. For Brownian motion of stationary and independent increments, the value of H is 0.5 and $D = 1.5$. This case can indicate that the coupled muscle groups are independent and are not recruited together. If H is greater than 0.5, *i.e.*, $1 < D < 1.5$, the interpretation is that the integrated effects of muscle groups can be categorized as positively correlated or persistent as in (20, 35). As shown in Fig. 1(A)–(E), the drastic drops of FDs from green to blue color code imply that the coupled muscle groups exhibit strong and persistent signal intensities. If D is between 1.5 and 2, the corresponding effect can be interpreted as negatively correlated or anti-persistent (20, 35). Notice that the covariance function of DFGN is also proportional to H and hence D according to equation [3]. Its corresponding covariance function is also proportional to signal intensity as indicated in (45). Consequently, D can be used as the first indicator of the persistence of "signal intensity" in the DFBM and DFGN models.

A second important indicator is the spectral frequency. To obtain the two indicators, D and spectral frequencies of surface EMG at the same time, a novel algorithm using spectral distribution function *via* DFGN was proposed (8, 10). The basic formulae were sketched below.

Spectral Distribution Function (SDF) (10)

Recall first that the harmonic representation of stationary signals can be given by the Bochner's theorem (16). For a continuous covariance function $r_H(\tau)$ on the real line, it can be represented in the form

$$r_H(\tau) = \int_{-\infty}^{\infty} e^{i2\pi\nu\tau} F(d\nu) \qquad [4]$$

where F is called the spectral measure. At points of continuity, it can be written as follows:

$$F([a, b]) = \lim_{n\to\infty} \int_{-\infty}^{\infty} r_H(\tau) \frac{e^{-i2\pi\tau b} - e^{-i2\pi\tau a}}{-i2\pi\tau} \cdot \exp[-\frac{1}{2}\frac{(2\pi\tau)^2}{n}] d\tau \,. \qquad [5]$$

In practice, for random sequences with the finite data length N and the real estimated $\hat{r}_H[n]$, the simplified formula of [5] can be written as follows:

$$\hat{F}(\lambda) = \hat{F}([0, \lambda]) = \frac{1}{2\pi}\hat{r}_H[0]\lambda + \frac{1}{2\pi}\sum_{n=1}^{N} \hat{r}_H[n]\frac{2\sin(\lambda n)}{n} \qquad [6]$$

where $\hat{F}(\lambda)$ is called the SDF induced by the spectral measure $F(\cdot)$. In practice, $\hat{F}(\lambda)$ is sampled at points $2\pi k/N$ and we denote the sampled $\hat{F}(\lambda)$ as $\hat{F}[k]$ for $k = 0, \cdots, N - 1$. The spectral frequency of any stationary sequence can then be obtained by taking the difference of SDF, and its corresponding FD can be calculated *via* equation [3].

Materials and Methods

Experimental Setup

Before the experiment, the skin in the right upper arm of a subject was abraded and then swabbed with alcohol to ensure a good condition of electrode contacts. The tested muscles of the upper arm included the biceps brachii, the brachialis, and the triceps brachii. Five pairs of disposable bipolar surface electrodes (Ag–AgCl, with 10 mm in diameter) were then attached to the subject's major flexors and extensors in the right upper arm. According to their anatomical surface markings, two pairs of them were attached to the short and long heads of biceps brachii (BBSH and BBLH), one to the brachialis (B), and two to the lateral and long heads of the triceps brachii (TBLTH and TBLH), respectively. The negative electrodes of these bipolar pairs were all placed at the belly regions of the corresponding muscle groups, the positive ones were placed at the proximal third, and the reference strip was placed near the right wrist. An electrogoniometer (SG110, Biometrics Ltd., Ladysmith, VA, USA.) was also taped on the lateral side of the forearm and upper arm to measure the flexion angle. The flexion angle was set to 0° when the elbow joint was fully extended and 90° when the forearm was perpendicular to the upper arm. After all these electrodes were placed and wired, the surface EMG signals were acquired by an MP150 system (Biopac Inc., Goleta, CA, USA). The gain of all amplifiers was set to 5000

and sampling rate at 2000 samples per second. In fact, the surface EMG activity of the right upper arm was actually below 250 Hz. Hence, the selected sampling rate was high enough for our experimental purposes. The signals were then filtered with a notch filter of 60 Hz to remove the power line effect and a band-pass filter (1-250 Hz).

Subjects and Experimental Protocols

Protocol 1: rest and volitional flexion of forearm. The range of ages in this group of six subjects was from 20 to 56 years with the distribution of 27.6 ± 14.2 (means ± SD) years. The range of heights was 171.4 ± 5.2 cm (means ± SD). All of them were right-handed and had no previous history of muscular injuries or myopathies in their right upper arms. Moreover, all of them gave their informed consent to this experiment. All experiments were approved by the National Tsing Hua University Ethical Committee. In this protocol, subjects were asked to lie down on a bed with palms and arms relaxed in supine position to minimize the muscular tension that might be resulted from the holding position of gestures during experiment. The experimental recordings began with a period of 30 s background rest data. This period of data could help us to make sure that the contact of electrodes was good and would be referred to as the background condition of the right upper arm later. After that period, subjects were asked to perform volitional flexion of their elbow joint without retraction. Meanwhile, an electronic metronome was set to beep every 4 s in order to coordinate their actions. For example, when hearing a beep sound, subjects were required to perform the flexion of their right upper arms by flexing their elbows voluntarily and smoothly within 4 s without any retraction. Then subjects were required to hold that posture. When hearing a second beep, subjects were required to recover the original posture by putting down their forearms smoothly as to be carried out by gravity. According to the data from electrogoniometer, the speed of vertical angle was kept around 85°/s to 100°/s. The combination of flexion and recovery motions was referred to as one flexion cycle in our experiment. Hence, the same flexion cycle was repeated at every two beeps. After 10 consecutive flexion cycles, subjects took a 180 s break to prevent muscular fatigue. Each subject was required to carry out a total of 30 cycles. To obtain data for control experiments, the following protocol was used.

Protocol 2: rest and passive flexion. The range of ages in this group of six subjects was from 20 to 55 years with the distribution of 28.5 ± 13.0 (means ± SD) years. The range of heights was 170.2 ± 4.6 cm (means ± SD). Thirty experiments for each person were performed on six healthy male subjects. All of them were right-handed and had no previous history of muscular injuries or myopathies in their right upper arms. Moreover, all of them gave their informed consent to this experiment and the experiments were approved by the National Tsing Hua University Ethical Committee. This group of subjects was age and gender matched with the group under protocol 1. Most parts of this protocol were the same as the previous one. The only difference was that each subject was passively flexed by an assistant instead of volitional flexion for 30 cycles.

Significant Peak Frequencies

To find the significant spectral frequencies during flexion, the following rules for significant peak frequencies found were adopted. For instance, in the surface EMG of short heads of biceps brachii, the maximal amplitude of the spectra during flexion was first identified. Then, the peak frequency whose amplitude was within 10 dB range of the maximal amplitude would be designated as significant. In addition, more than five significant frequencies were allowed for each flexion as long as they could satisfy the aforementioned criterion. As a result, we would not miss any significant frequencies if they were indeed present. The other four channels were also treated in the same way.

Analysis Method for Surface EMG Signals

The data were analyzed using the Matlab (MathWorks Inc., Natick, MA, USA) software package running on an IBM compatible PC. In this paper, a window size of 1 s (2000 samples) was selected to perform the estimations of the Hurst parameter H and spectral frequency. After obtaining the Hurst parameter H and spectral frequency of the first window, we then shifted the window to the right by 0.05 second (100 sample points) and calculated the H and spectral frequency of the next window. These steps were repeated until the end of time series. With this window size, the resolution of the spectrum was limited to 1 Hz. After using this sliding window analysis, the sequences of Hurst parameter and spectral frequency of the signals were obtained. Notice that the range of H is from 0 to 1 and the FD is then obtained by $D = 2 - H$.

Statistical Analysis

The results of statistical analysis in this paper were presented in means ± SEM (standard error of the mean). Statistical significant difference was tested using two-tailed t-test for unpaired data. Statistical outcomes were regarded as significant when $P < 0.01$. For instance, the null hypothesis that the means of two groups of data were the same would be rejected

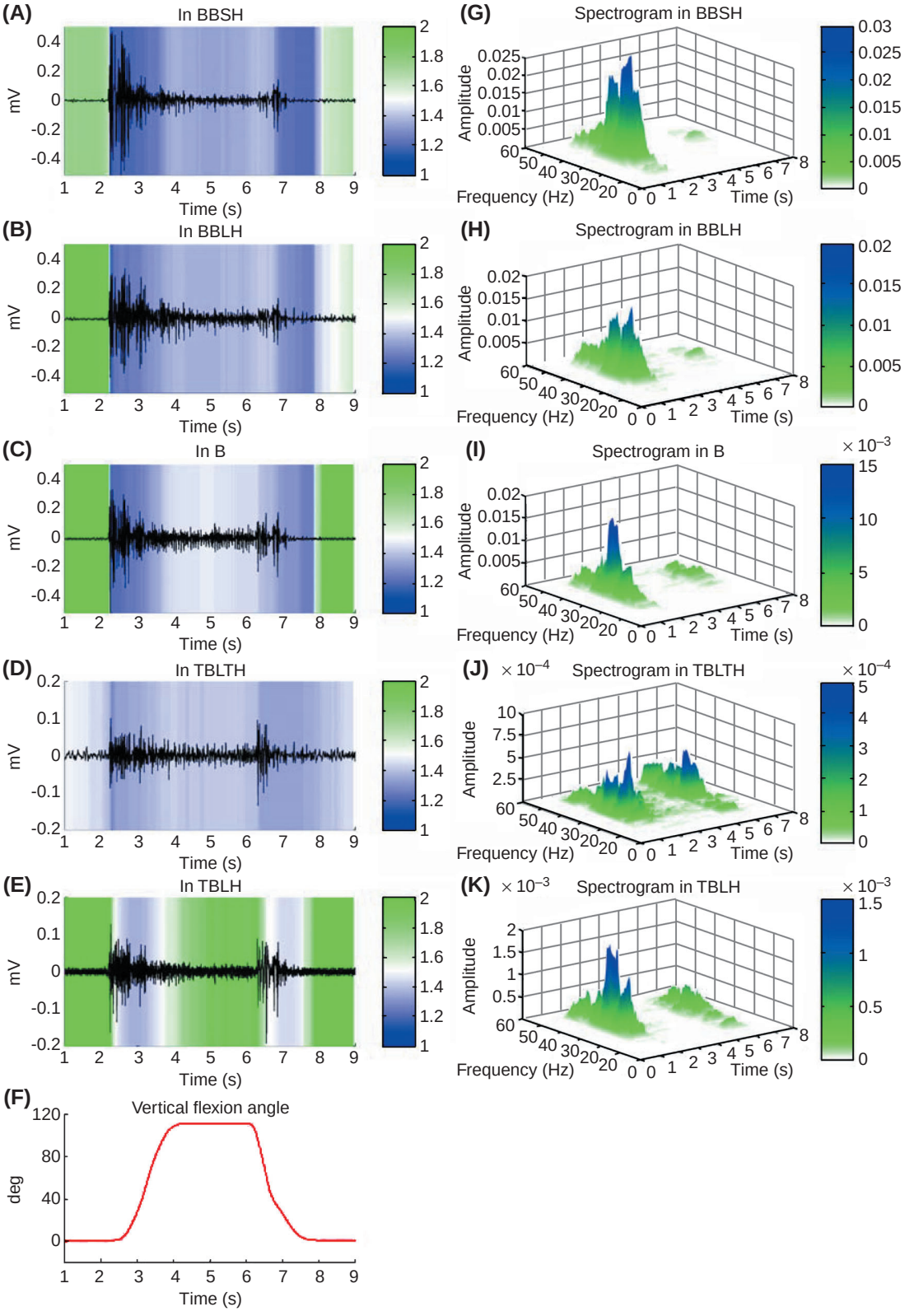

Fig. 1. Surface EMG activities, temporal FDs, and spectrograms of five different brachial muscles of a right upper arm during one exemplary flexion cycle. The activities of surface EMG in dark color and temporal FDs in color codes for muscles of BBSH (A), BBLH (B), B (C), TBLTH (D), and TBLH (E), respectively. The corresponding spectrograms for these muscles are presented from (G) to (K), respectively. The elbow flexion angle in the Y axis from electrogoniometer is presented in (F). The metronome beeps at 2 s to instruct the subject to flex and at 6 s to instruct the subject to extend. The FD means during rest and flexion are summarized in Table 1.

when $P < 0.01$.

Results

One Complete Elbow Flexion Cycle under Protocol 1

The surface EMG activities, temporal FDs, and spectrograms of five parts of the brachial muscles of subject 1 during one exemplary flexion cycle were displayed in Fig. 1. The typical surface EMG signals were depicted in black color. The temporal FDs were denoted by color codes. For instance, in Fig. 1A, the surface EMG activity of BBSH was exhibited in black color. The dark blue patterns (with FDs around 1.2 to 1.3) within the range of 2.2 to 3.5 s corresponded to the flexion of the BBSH by flexing only the elbow. Then, the light blue patterns (with FDs around 1.4 to 1.5) around the range of 3.5 to 6.9 s corresponded to an isometric contraction of the holding position. Finally, the medium blue patterns (with FDs around 1.3 to 1.4) around the range of 6 to 8 s corresponded to the period of putting down forearm smoothly by gravity. The spectral frequencies of the corresponding BBSH muscle were depicted in Fig. 1G. The three high peak values in this exemplary elbow flexion were located around 24, 27, and 34 Hz. The vertical flexion angle of the elbow joint from electrogoniometer was displayed in Fig. 1F. Similarly, the surface EMG activities and spectrograms of BBLH, B, TBLTH, and TBLH were represented in Fig. 1, B-E and H-K, respectively.

Of the muscular activities during flexion, all their FDs were less than 1.5 in this period. This result could be seen from Fig. 1, A-E as the color codes all changed from green to blue. Moreover, all five parts of the brachial muscles within the range of 2.2 to 3.5 s had three high peak values around 24, 27, and 34 Hz in this exemplary elbow flexion. During the holding period (3.5 to 6.9 s), we could see that all am-plitudes of the spectra were quite small when compared with those in the flexion period even though the FDs were still in the blue region except the relatively weak TBLH. In addition, during the period of putting down the forearm smoothly by gravity (6.9 to 8 s), we could see that all muscles exhibited lower FDs (< 1.5), even though all amplitudes of the spectra were smaller than those in the flexion period. However, this period is not our focus in this paper. Finally, the statistical results in Table 1 indicated that there were significant differences between the mean values of FDs for the five parts of brachial muscles during rest and those during elbow flexion ($P < 0.01$).

Control Experiments under Protocol 2

All experiments under protocol 2 were similar and one typical control experiment in which the subject was passively flexed was demonstrated in Fig. 2. No apparent bursting activities were observed for all the muscles except B around 3 s. Their spectral amplitudes of surface EMGs remained small and no prominent frequencies were found during the whole procedure. Moreover, their FDs did not exhibit change of color codes from green to blue as in volitional flexion ($P > 0.05$). The other flexions in control experiments were similar and had no statistically significant differences.

Table 1. A comparison of the mean FDs of the brachial muscles of subject 1 during rest versus elbow flexion. Values (means ± SEM , n = 20) are calculated from the trial in Fig. 1. Here, n is the number of the FD values used. Means during flexion are separable from those during rest with $P < 0.01$. BBSH and BBLH stand for the short and long heads of biceps brachii, respectively. B stands for the brachialis. TBLTH and TBLH stand for the lateral and long heads of the triceps brachii, respectively

Muscle Groups	Rest	Flexion
BBSH	1.74 ± 0.02	1.20 ± 0.02
BBLH	1.97 ± 0.01	1.26 ± 0.03
B	1.99 ± 0.01	1.26 ± 0.04
TBLTH	1.47 ± 0.02	1.35 ± 0.03
TBLH	1.99 ± 0.01	1.40 ± 0.04

Synchronized Significant Peak Frequencies in Both Protocols

To further examine the synergic information contained in the spectrograms of all five parts of the brachial muscles, we identified the significant peak frequencies of protocol 1 in Fig. 1. The results indicated that three significant peak frequencies, namely, 24, 27, and 34 Hz, concurrently showed up in all five groups of brachial muscles during flexion (see Fig. 3A). Thus, a special name was given to these frequencies: the "synchronized" significant peak frequencies (SSPFs). In this study, the resolution of our power spectrum was limited to 1 Hz. Hence, significant peak frequencies could drift by 1 Hz due to the resolution or instrument noise.

In Fig. 3B, the same criteria for finding significant peak frequencies were also applied to the control experiment of protocol 2 in Fig. 2. However, results indicated that the frequencies of each muscle group were very small in magnitude and there were no SSPFs observed for all five muscle groups. As a matter of fact, all control experiments of protocol 2

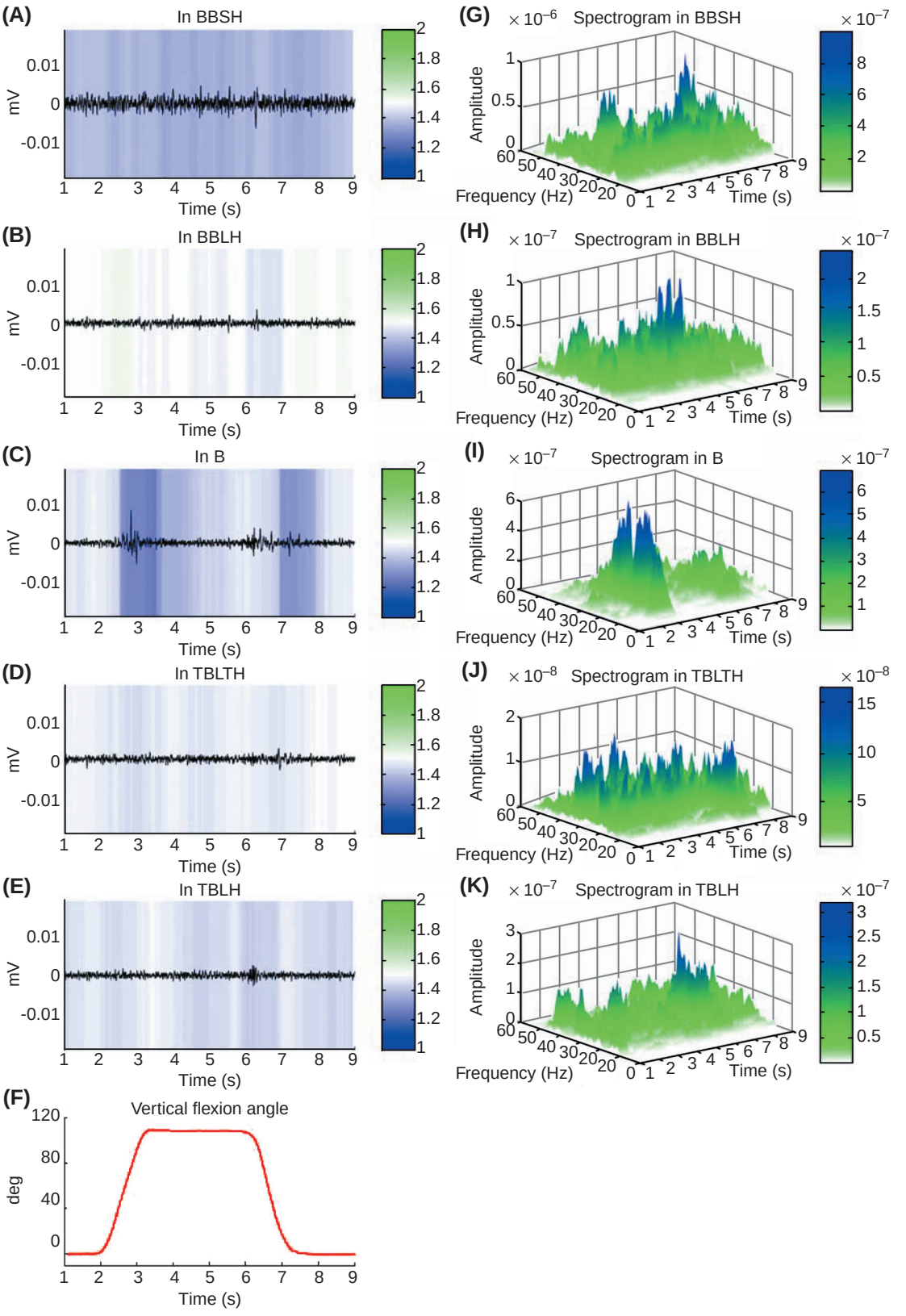

Fig. 2. Surface EMG activities, temporal FDs, and spectrograms of five different brachial muscles of a right upper arm during one control experiment. The activities of surface EMG in dark color and temporal FDs in color codes for muscles of BBSH (A), BBLH (B), B (C), TBLTH (D), and TBLH (E), respectively. The corresponding spectrograms for these muscles are presented from (G) to (K), respectively. The elbow flexion angle in vertical axis from electrogoniometer is presented in (F). The metronome beeps at 2 s to instruct the assistant to flex the subject's elbow joint and at 6 s to extend.

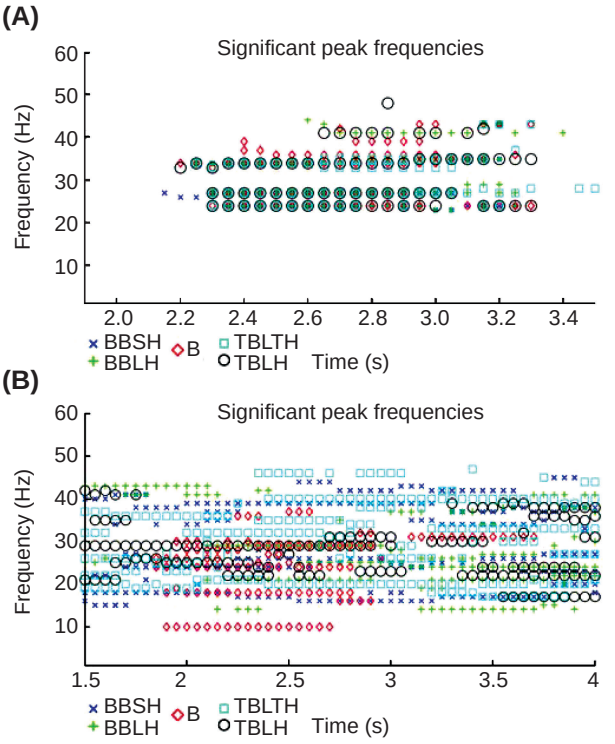

Fig. 3. Significant synchronization peak frequencies (SSPFs) of brachial muscles during elbow flexion of Fig. 1 and control experiment of Fig. 2. (A) The SSPFs of each muscle during flexion are marked according to the symbols shown in the lower left corner. All five muscles are synchronized around 24, 27, and 34 Hz. (B) No SSPFs are found.

exhibited similar types of behavior and no statistically significant result was obtained.

Synchronized Significant Peak Frequencies and FDs of 6 Subjects under Protocol 1

So far we verified that the rhythms of the five parts of muscles were all synchronized and the FDs were temporally persistent during one exemplary flexion cycle under protocol 1. However, to get the dynamical behavior of all cycles, the SSPFs of each cycle and the averaged temporal FDs of 30 cycles were exhibited in Fig. 4. The SSPFs that were present in *all* five parts of the brachial muscles during flexions (Fig. 4, A-F) were denoted in heavy dots. The results turned out that each flexion could have two, three or four different SSPFs. These 30 cycles for each subject were arranged according to the SSPFs. The averaged temporal FDs of the corresponding 30 trials were also presented in Fig. 4, G-L. From Fig. 4, we observed that these averaged FD values of flexors and extensors of the 6 subjects dropped simultaneously during flexion. There was similar behavior in extension, but it was not our main focus at present.

Table 2. Comparison of the mean FDs of the brachial muscles during rest versus elbow flexion for six subjects. Values (means ± SEM, n = 600) are calculated from each part of the muscles during rest versus elbow flexion. The mean values during flexion are separable from those during rest with $P < 0.01$. Here, n = 600 comes from 30 cycles and each cycle with 20 FD values. The abbreviations of muscle groups are in the caption of Table 1

Subjects	Muscle Groups	Rest	Flexion
Subject 1	BBSH	1.65 ± 0.09	1.21 ± 0.03
	BBLH	1.80 ± 0.20	1.26 ± 0.04
	B	1.98 ± 0.05	1.27 ± 0.05
	TBLTH	1.44 ± 0.03	1.34 ± 0.03
	TBLH	1.98 ± 0.01	1.40 ± 0.04
Subject 2	BBSH	1.71 ± 0.22	1.23 ± 0.03
	BBLH	1.78 ± 0.16	1.22 ± 0.03
	B	1.56 ± 0.07	1.38 ± 0.03
	TBLTH	1.86 ± 0.20	1.33 ± 0.09
	TBLH	1.74 ± 0.28	1.35 ± 0.05
Subject 3	BBSH	1.70 ± 0.10	1.28 ± 0.07
	BBLH	1.53 ± 0.04	1.24 ± 0.05
	B	1.62 ± 0.07	1.31 ± 0.06
	TBLTH	1.51 ± 0.03	1.28 ± 0.05
	TBLH	1.53 ± 0.03	1.39 ± 0.04
Subject 4	BBSH	1.48 ± 0.05	1.35 ± 0.03
	BBLH	1.51 ± 0.05	1.33 ± 0.03
	B	1.53 ± 0.02	1.41 ± 0.03
	TBLTH	1.52 ± 0.02	1.44 ± 0.03
	TBLH	1.49 ± 0.01	1.43 ± 0.03
Subject 5	BBSH	1.50 ± 0.14	1.29 ± 0.04
	BBLH	1.45 ± 0.05	1.26 ± 0.03
	B	1.53 ± 0.04	1.26 ± 0.04
	TBLTH	1.53 ± 0.11	1.33 ± 0.08
	TBLH	1.45 ± 0.05	1.33 ± 0.05
Subject 6	BBSH	1.87 ± 0.21	1.30 ± 0.08
	BBLH	1.81 ± 0.26	1.28 ± 0.07
	B	1.77 ± 0.19	1.34 ± 0.07
	TBLTH	1.84 ± 0.17	1.33 ± 0.07
	TBLH	1.40 ± 0.07	1.41 ± 0.03

The statistical results (Tables 2 and 3) indicated that there were significant differences between the rest and the flexion state for each individual and the whole group by $P < 0.01$.

Discussion

Synergic Co-Activation of Muscles during Elbow Flexion under Protocol 1

The primary new finding from this study is that

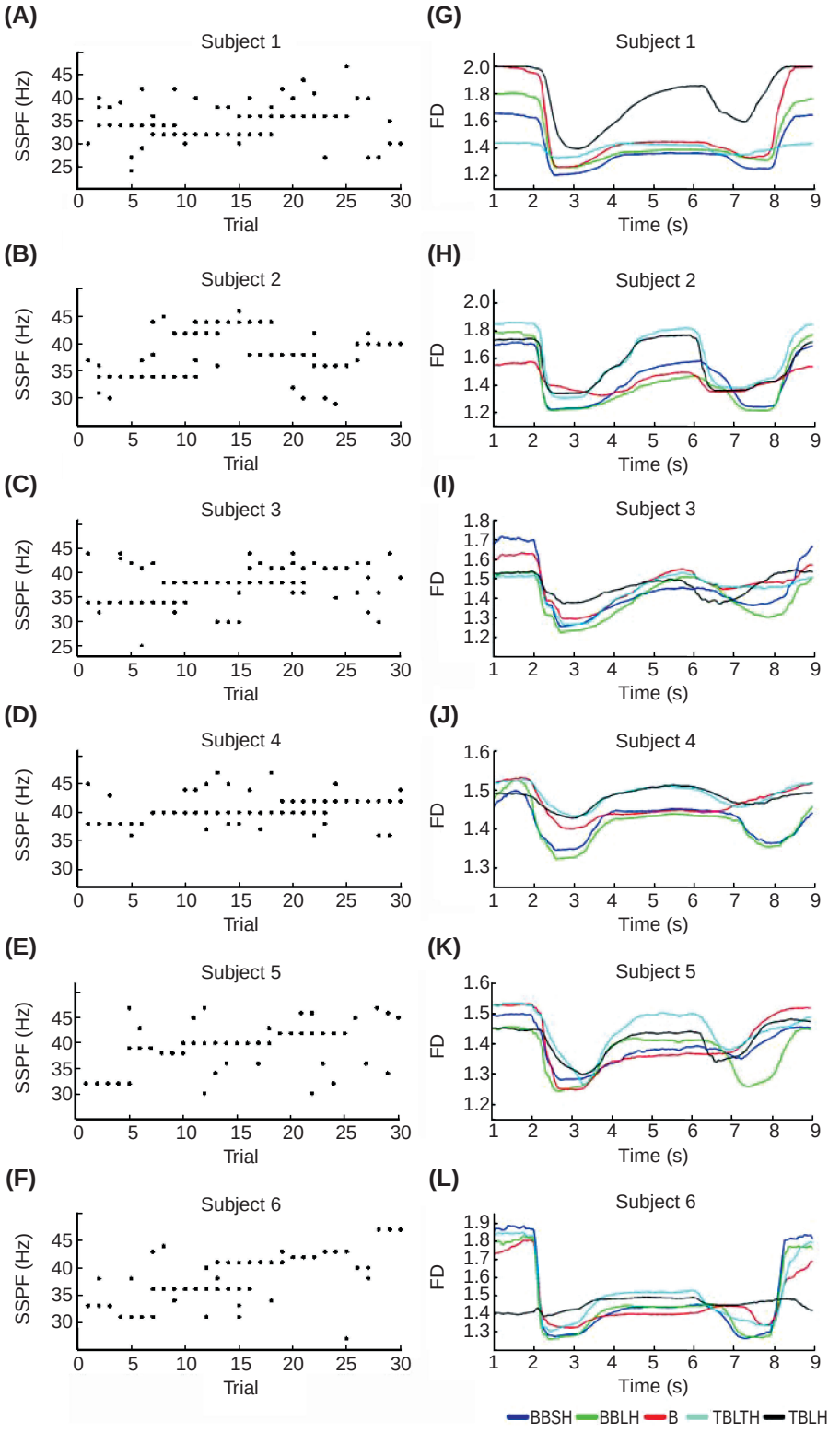

Fig. 4. The synergy of brachial muscles *via* coherent temporal FDs and SSPFs for the 6 subjects. (A)-(F): The SSPFs of each trial for the 6 subjects. (G)-(L): The averaged temporal FDs out of 30 trials for each subject, respectively. Different trials are aligned according to the beep sound at 2 s in order to average the FDs. Statistical means ± SEM are summarized in Table 2.

all five parts of the brachial muscles in the upper arm are under synergic co-activation during flexion. The reasons are twofold. First of all, from the color codes (Fig. 1, A-E), all the muscle groups simultaneously drop to the dark blue region (FDs around 1.2 to 1.4) within the range of 2.2 to 3.5 s for the exemplary

Table 3. Group comparison of the mean FDs. Values (means ± SEM, n = 3600) are calculated from each part of the muscles during rest versus elbow flexion. The mean values during flexion are separable from those during rest with $P < 0.01$. Here, n is the number of the FD values and n = 3600 comes from 6 subjects and each with 600 values. The abbreviations of muscle groups are in the caption of Table 1

Muscle Groups	Rest	Flexion
BBSH	1.65 ± 0.20	1.28 ± 0.07
BBLH	1.65 ± 0.22	1.27 ± 0.06
B	1.67 ± 0.19	1.33 ± 0.07
TBLTH	1.62 ± 0.20	1.34 ± 0.08
TBLH	1.60 ± 0.24	1.38 ± 0.06

flexion cycle. Meanwhile, the average values of FDs can be separated statistically from those during rest (Table 1). These results indicate that the signal intensities of these muscle groups are "persistent" or "positively correlated" simultaneously during flexion. Secondly, all five spectrograms in Fig. 1, G-K present the same SSPFs around 24, 27 and 34 Hz. The three synchronized frequencies for all five groups of muscles are explicitly indicated in Fig. 3A. Notice that these two afore-mentioned phenomena are all absent during the control experiments of protocol 2 in Fig. 2 and Fig. 3B. Combining these two experimental facts on frequency synchronization and temporal persistence of muscle groups *via* FDs, we can agree that these coupled muscle groups work together with the same frequencies and significant intensities to facilitate an efficient and smooth flexion. Therefore, the results of Figs. 1 and 3A indicate that in this exemplary flexion, the five muscle groups are synergically co-activated with synchronized rhythms.

Notice that the effects of crosstalk among different surface EMGs are insignificant in our experimental design and results. The reasons are threefold. First, the electrodes are carefully separated at the outset. Secondly, from the control experiment, a relatively large surface EMG activity (2 to 4 s) is observed in the flexion of B (Fig. 2C), yet it has not affected the other adjacent muscles (Fig. 2, A-B and D-E) during the same time. This phenomenon demonstrates that with such electrode configuration the crosstalk is negligible in the data recording. Thirdly, the bursting activities of all tested muscle groups during volitional flexion (Fig. 1, A-E) are large and comparable in magnitude. This means that these activities cannot be derived solely from crosstalk since crosstalk signals are in general attenuated in magnitude due to spatial filtering effect (33, 41, 47).

As for Fig. 4, A-F, it is understandable that different SSPFs exist for different subjects and even different cycles of the same subject. However, two things remain to be true. That is, all coupled muscle groups must be synchronized in frequencies during flexion. In addition, the averaged temporal FDs of the 30 cycles for all muscle groups are persistent as displayed in Fig. 4, G-L. Notice that a simultaneous drop of FDs during flexion is observed for all subjects. All the values of FDs are way under 1.5 during flexion. Besides, the mean values of FDs can also be separated statistically from those during rest with $P < 0.01$ (Table 2). Combining the results of FDs and synchronization of rhythms, we see again that all muscle groups are working synergically during flexion. This fact is now consistent in 180 cycles. Moreover, by the group comparison (Table 3), it is also true for different subjects with $P < 0.01$.

Based on these experimental findings, the involved muscles during volitional flexion indeed work together synergically. The synergic co-activation of them is believed to facilitate the movement. This way, resistance of the motion will be reduced and the production of quick and smooth movement will follow. Finally, we would like to mention that the reciprocal inhibition has not been observed in this study. One possible explanation is that the nerve cells and fibers in our experiment were not stimulated by strong induction shock; hence hyperpolarization would not be induced.

In conclusion, we have confirmed that the five coupled muscle groups in the upper arm are synergically co-activated during elbow flexion by using the SSPFs and temporal FDs as two important quantitative indicators. It is believed that these coupled muscle groups have to work together to facilitate flexion. On the other hand, the phenomenon of reciprocal inhibition has not been observed in this study. It will be interesting to study in the future why the reciprocal inhibition has not occurred.

Acknowledgments

This work was supported under the Grant number NSC 97-2221-E-007-072 of National Science Council, Taiwan, Republic of China.

References

1. Barrington, F.J.F. The component reflexes of micturition in the cat. *Brain* 54: 177-188, 1931.
2. Barrington, F.J.F. The nervous mechanism of micturition. *Quart. J. Exp. Physiol.* 8: 33-71, 1914.
3. Breteler, M.D.K., Simura, K.J. and Flanders, M. Timing of muscle activation in a hand movement sequence. *Cerebral Cortex* 17: 803-815, 2007.
4. Buchanan, T.S., Rovai, G.P. and Rymer, W.Z. Strategies for

muscle activation during isometric torque generation at the human elbow. *J. Neurophysiol*. 62: 1201-1212, 1989.
5. Busse, M.E., Wiles, C.M. and Deursen, R.W.M.V. Muscle co-activation in neurological conditions. *Phys. Ther. Rev*. 10: 247-252, 2005.
6. Caldwell, G.E., Jamison, J.C. and Lee, S. Amplitude and frequency measures of surface electromyography during dual task elbow torque production. *Eur. J. Appl. Physiol. Occup. Physiol*. 66: 349-356, 1993.
7. Chang, S., Chiang, M.J., Li, S.J., Hu, S.J., Cheng, H.Y., Hsieh, S.H. and Cheng, C.L. The Cooperative Phenomenon of Autonomic Nervous System in Urine Storage. *Chinese J. Physiol*. 52, 2009 (in press)
8. Chang, S., Hsyu, M.J., Cheng, H.Y. and Hsieh, S.H. Synergic co-activation in forearm pronation. *Ann. Biomed. Eng.* 36: 2002-2018, 2008.
9. Chang, S., Hu, S.J. and Lin, W.C. Fractal dynamics and synchronization of rhythms in urodynamics of female Wistar rats. *J. Neurosci. Meth.* 139: 271-279, 2004.
10. Chang, S., Li, S.J., Chiang, M.J., Hu, S.J. and Hsyu, M.C. Fractal dimension estimation *via* spectral distribution function and its application to physiological signals. *IEEE Trans. Biomed. Eng*. 53: 1895-1898, 2007.
11. Chang, S., Mao, S.T., Hu, S.J., Lin, W.C. and Cheng, C.L. Studies of detrusor-sphincter synergia and dyssynergia during micturition in rats via fractional Brownian motion. *IEEE Trans. Biomed. Eng.* 47: 1066-1073, 2000.
12. Chang, S., Mao, S.T., Kuo, T.P., Hu, S.J., Lin, W.C. and Cheng, C.L. Fractal geometry in urodynamics of lower urinary tract. *Chinese J. Physiol*. 42: 25-31, 1999.
13. Cheng, C.L., Chai, C.Y. and de Groat, W.C. Detrusor-sphincter dyssynergia induced by cold stimulation of the urinary bladder of rats. *Am. J. Physiol*. 272: R1271-1282, 1997.
14. d'Avella, A. and Bizzi, E. Shared and specific muscle synergies in natural motor behaviors. *Proc. Natl. Acad. Sci. U.S.A*. 102: 3076-3081, 2005.
15. d'Avella, A., Saltiel, P. and Bizzi, E. Combinations of muscle synergies in the construction of a natural motor behavior. *Nat. Neurosci.* 6: 300-308, 2003.
16. Doob, J.L. Stochastic processes, New York, Wiley, 1953.
17. Dupont, L., Gamet, D. and Perot, C. Motor unit recruitment and EMG power spectra during ramp contractions of a bifunctional muscle. *J. Electromyogr. Kinesiol*. 10: 217-224, 2000.
18. Ehtiati, T. and Kinsner, W. Multifractal characterization of electromyogram signals. In: Proceedings of the 1999 IEEE Canadian Conference on Electrical and Computer Engineering, pp. 792-796, 1999.
19. Farina, D., Merletti, R. and Enoka, R.M. The extraction of neural strategies from the surface EMG. *J. Appl. Physiol*. 96: 1486-1495, 2004.
20. Feder, J. Fractals, New York and London, Plenum Press, 1988.
21. Frysinger, R.C., Bourbonnais, D., Kalaska, J.F. and Smith, A.M. Cerebellar cortical activity during antagonist cocontraction and reciprocal inhibition of forearm muscles. *J. Neurophysiol*. 51: 32-49, 1984.
22. Gielen, C.C. and van Zuylen, E.J. Coordinations of arm muscles during flexion and supination: Application of the tensor analysis approach. *Neuroscience* 17: 527-539, 1986.
23. Gitter, J.A. and Czerniecki, M.J. Fractal analysis of the electromyographic interference pattern. *J. Neurosci. Meth*. 58: 103-108, 1995. 25
24. Glass, L. Synchronization and rhythmic processes in physiology. *Nature* 410: 277-284, 2001.
25. Goldberger, A.L., Amaral, L.A.N., Hausdorff, J.M., Ivanov, P.C., Peng, C.K. and Staley, H.E. Fractal dynamics in physiology: Alternations with disease and aging. *Proc. Natl. Acad. Sci. U.S.A.* 99: 2466-2472, 2002.
26. Gupta, V., Suryanarayanan, S. and Reddy, N.P. Fractal analysis of surface EMG signals from the biceps. *Int. J. Med. Inform*. 45: 185-192, 1997.
27. Hannaford, B. and Steven, L. Short time fourier analysis of the electromyogram -fast movements and constant contraction. *IEEE Trans. Biomed. Eng*. 33: 1173-1181, 1986.
28. Hasan, Z. and Enoka, R.M. Isometric torque-angle relationship and movement-related activity of human elbow flexors: implications for the equilibrium-point hypothesis. *Exp. Brain Res*. 59: 441-450, 1985.
29. Hwang, I.S. and Abraham, L.D. Quantitative EMG analysis to investigate synergistic coactivation of ankle and knee muscles during isokinetic ankle movement. Part 2: time frequency analysis. *J. Electromyogr. Kinesiol*. 11: 327-335, 2001.
30. Jamison, J.C. and Caldwell, G.E. Muscle synergies and isometric torque production: influence of supination and pronation level on elbow flexion. *J. Neurophysiol*. 70: 947-960, 1993.
31. Lee, D.D. and Seung, H.S. Learning the parts of objects by non-negative matrix factorization. *Nature* 401: 788-791, 1999.
32. Liu, S.C. and Chang, S. Dimension estimation of discrete-time fractional Brownian motion with applications to image texture classification. *IEEE Trans. Image Process* 6: 1176-1184, 1997.
33. De Luca, C.J. The use of surface electromyography in biomechanics. *J. Appl. Physiol*. 13: 135-163, 1997.
34. MacIsaac, D.T., Parker, P.A. and Scott, R.N. Examining the mean frequency of myoelectric signals produced by dynamic muscle contractions. In: Proceedings of the 20th Annual International Conference of the IEEE Engineering in Medicine and Biology Society. vol. 20: pp. 2650-2653, 1998.
35. Mandelbrot, B.B. The Fractal Geometry of Nature, San Francisco, Freeman, 1982.
36. Naito, A. Electrophysiological studies of muscles in the human upper limb: the biceps brachii. *Anat. Sci. Int.* 79: 11-20, 2004.
37. Naito, A., Sun, Y.J., Yajima, M., Fukamachi, H. and Ushikoshi, K. Electromyographic study of the elbow flexors and extensors in a motion of forearm pronation/supination while maintaining elbow flexion in humans. *Tohoku J. Exp. Med*. 186: 267-277, 1998.
38. Paley, R.E.A.C. and Wiener, N. Fourier Transforms in the Complex Domain, American Mathematical Society Providence, R. I., 1934.
39. Shefchyk, S.J. Sacral spinal interneurones and the control of urinary bladder and urethral striated sphincter muscle function. *J. Physiol*. 533: 57-63, 2001.
40. Sherrington, C.S. The Integrative Action of the Nervous System, London, Cambridge Univ. Press, 1906.
41. Solomonow, M., Baratta, R.V., Zhou, B.H., Bernardi, M. and Acierno, S. Analysis of EMG crosstalk in neighboring and antagonist cat muscles. In: Engineering in Medicine and Biology Society, 1995. IEEE 17th Annual Conference, 1995, pp. 1353-1354.
42. Standring, S. Gray's Anatomy, New York, Churchill Livingstone, 2005.
43. Tresch, M.C., Saltiel, P. and Bizzi, E. The construction of movement by the spinal cord. *Nat. Neurosci*. 2: 162-167, 1999.
44. van Zuylen, E.J., Gielen, C.C. and Denier van der Gon, J.J. Coordination and inhomogeneous activation of human arm muscles during isometric torques. *J. Neurophysiol.* 60: 1523-1548, 1988.
45. Voss, R. The Science of Fractal Images. In: *Fractals in Nature: From Characterization to Simulation*, edited by Peitqen, H.O. and Saupe, D. New York Springer-Verlag, 1988, pp. 21-70.
46. Walsh, P.C., Retik, A.B. and Vaughan, E.D. Campbell's Urology, Philadelphia, Saunders, 2002.
47. Winter, D.A., Fuglevand, A.J. and Archer, S.E. Crosstalk in surface electromyography: theoretical and practical estimates. *J. Electromyogr. Kinesiol*. 4: 15-26, 1994.